

Optimization of probability model for color halftone by macroscopic spectral reflectance

*Akihiro Ito and Noboru Ohta**

Fuji Xerox Co., Ltd.

Ebina, Kanagawa, Japan

**Munsell Color Science Laboratory*

Chester F. Carlson Center for Imaging Science

Rochester Institute of Technology

Rochester, New York, USA

Abstract

In order to improve the Yule-Nielsen effect, a variety of models have been proposed. The probability model is one of them, and it describes the effect based on real physical structures. However when the model is used for color halftone, colorimetric measurements of image microstructure are needed. In the present study, we assume that a dot area fraction F and a probability function P in the probability model are independent of wavelength. Then we have derived these parameters from macroscopic spectral reflectance measurements.

Introduction

The overall reflectance factor, R , of a halftone image is modeled by the Murray-Davies equation:

$$R = F \cdot R_i + (1-F) \cdot R_p \quad (1)$$

where F is the fractional area coverage of the ink dots, and R_i and R_p are the reflectance factors of the ink and paper, respectively. However, when fixed values are used for R_i and R_p , typically an actual measured value of R indicates nonlinear relationship with F , and it is darker than predicted by Eq. 1. This phenomenon is mainly caused by the lateral scattering of light within the paper and is called the Yule-Nielsen effect, or optical dot gain.

Huntsman modeled the Yule-Nielsen effect from considerations of photon behavior within the paper.¹ He considered that a part of the photons that entered from the paper between the dots emerged under the dots, and vice versa. He traced each route of the photons, and made the model. Therefore, when the fraction of the photons that take each route are found out, R that includes the Yule-Nielsen effect can be derived. This model was arranged by Arney as probability function and he expressed the probability by function of F value.^{2,3,4} To optimize the probability model, F , R_i , and R_p are measured by a

microdensitometer. However, the microdensitometer doesn't have easy handling. Especially for colorimetric measurement, correction of the instrument and treatment for measured data are very difficult.

We attempted to derive the parameters for the probability model from the macroscopic spectral reflectance measurements instead of the microscopic reflectance measurements.

Experimental

Basic Theory

In Eq. 1, R_i and R_p are not fixed values. They vary according to F value. For two regions, region0 (paper) and region1 (ink), there are four probability functions, P_{00} , P_{01} , P_{11} , and P_{10} . P_{00} is the probability of the photons that entered from region0 will emerge from region0, and P_{01} , P_{11} , and P_{10} are similar. Tracing each route and applying reflectance and transmittance factor on the route, Eq. 2 and Eq. 3 can be derived:^{2,3}

$$R_p = R_g \cdot T_0 \cdot (T_0 \cdot P_{00} + \frac{F}{1-F} \cdot T_1 \cdot P_{10}) \quad (2)$$

$$R_i = R_g \cdot T_1 \cdot (T_1 \cdot P_{11} + \frac{1-F}{F} \cdot T_0 \cdot P_{01}) \quad (3)$$

where T_0 and T_1 are the transmittance factors of the ink in region0 and region1 respectively and R_g is the reflectance factor of the un-printed paper. If there is no ink in region0, T_0 is 1. Furthermore, considering symmetry property of scattering, the number of parameters can be reduced as Eq. 4, Eq. 5 and Eq. 6:³

$$R_p = R_g \cdot T_0 \cdot (P_{00} \cdot (T_0 - T_1) + T_1) \quad (4)$$

$$R_i = R_g \cdot T_1 \cdot (P_{11} \cdot (T_1 - T_0) + T_0) \quad (5)$$

$$P_{00} = 1 - (1 - P_{11}) \cdot \frac{F}{1 - F} \quad (6)$$

Because an electrophotographic printer uses toner that has a tendency to scatter light, instead of Beer-Lambert transmittance, using the Kubelka-Munk absorption and scattering for the electrophotographic printer were suggested by Arney and Tsujita⁵. Eq. 7 is one of the Kubelka-Munk formulas. The reflectance factor at $F=1$, R_{min} , can be modeled with the Kubelka-Munk absorption and scattering coefficients of the toner, K and S , R_g , and the toner layer thickness at $F=1$, x :⁶

$$R_{min} = \frac{1 - R_g \cdot [a - b \cdot \coth(b \cdot S \cdot x)]}{a - R_g + b \cdot \coth(b \cdot S \cdot x)} \quad (7)$$

where $a=K/S+1$ and $b=(a^2-1)^{1/2}$. Solving Eq. 7 for Sx , Eq. 8 can be obtained:

$$S \cdot x = \frac{\coth^{-1}\left(\frac{1 - a \cdot R_g - a \cdot R_{min} + R_g \cdot R_{min}}{b \cdot (R_{min} - R_g)}\right)}{b} \quad (8)$$

$$T_{km} = \frac{b}{a \cdot \sinh(b \cdot S \cdot x) + b \cdot \cosh(b \cdot S \cdot x)} \quad (9)$$

$$R_{km} = \frac{1}{a + b \cdot \coth(b \cdot S \cdot x)} \quad (10)$$

Eq. 9 and Eq. 10 are also Kubelka-Munk formulas. Using Eq. 8, Eq. 9, and Eq. 10, the Kubelka-Munk transmittance factor of the toner, T_{km} , the reflectance factor of the toner with a black backing material, R_{km} can be obtained. For the opaque toner system, we reconsidered each route of the light, and we modified Eq. 4 and Eq. 5 as following:

$$R_p = P_{00} \cdot (R_{KM0} + \frac{T_{KM0}^2 \cdot R_g}{1 - R_{KM0} R_g}) + (1 - P_{00}) \cdot \frac{T_{KM1}}{1 - R_{KM1} R_g} \cdot \frac{T_{KM0} R_g}{1 - R_{KM0} R_g} \quad (11)$$

$$R_i = P_{11} \cdot (R_{KM1} + \frac{T_{KM1}^2 R_g}{1 - R_{KM1} R_g}) + (1 - P_{11}) \cdot \frac{T_{KM0}}{1 - R_{KM0} R_g} \cdot \frac{T_{KM1} R_g}{1 - R_{KM1} R_g} \quad (12)$$

where T_{km0} and T_{km1} are T_{km} in region0 and region1, R_{km0} and R_{km1} are R_{km} in region0 and region1, respectively. When there is no toner in region0, T_{km0} is 1 and R_{km0} is 0.

R_g , R_{min} and K/S of the toner can be measured easily. Therefore, using Eq. 8, Eq. 9, and Eq. 10, T_{km} and R_{km} can be obtained. If P_{00} and F can be obtained, using Eq. 11, Eq. 12, and Eq. 1, the overall reflectance factor R can be obtained. In the previous work, F , R_p , and R_i were measured by the microdensitometer, and the model to express the relationship between F and P_{11} were made.

Optimization by Spectral Reflectance Factor

If all measurements, R , R_{min} , R_g , and K/S are measured as spectral, for example 400nm to 700nm at intervals of 10nm, 31 data can be obtained for each variable. On the other hand, the dot size never varies even though it is observed by different wavelength light. Therefore, the same value can be used for F value at each wavelength, and

also for P_{00} value. This means 31 sets of Eq. 1, Eq. 11, and Eq. 12 can be obtained from the measurement of one sample. And they include only two unknown variables, F and P_{11} . Using a nonlinear optimization method, the optimum F and P_{11} values should be obtained.

A system of Fuji Xerox Acolor936 and SM ICS was used in this research. This system works as an electrophotographic PostScript printer and has a hybrid screen system for a pictorial image. The hybrid screen consists of a 200lpi line screen and 100dpi cluster dot screen, and the cluster dot screen is used in highlight area. Cyan ramp patch samples, $F_c=0.0, 0.2, 0.3, 0.4, 0.5, 0.6, 0.7, 0.8, 0.9$, and 1.0, were printed by the system. F_c is the value commanded by the printer. The cluster dot screen was used for only $F_c=0.2$ sample. The samples were measured using Gretag SPM60 spectrophotometer with a black backing material. This instrument has 45/0-degree geometry and 3.5mm aperture size.

The Simplex method with root-mean-square (RMS) of reflectance error through each wavelength as an evaluation function was used as the nonlinear optimization method. And F and P_{11} of each patch were optimized separately. However, because this optimization has many local minimum values, the result depends on an initial value given to the Simplex method. Therefore it was necessary to decide an appropriate initial value before using the Simplex method. To decide the appropriate initial value, all combinations of F and P_{11} at intervals of 0.01 were calculated and the best combination of F and P_{11} that obtained the best value from the evaluation function was used as the initial values for the Simplex method.

Figure 1 shows optimized F (solid line) and P_{11} (dotted line). Using Eq. 1, Eq. 11, Eq. 12, and the optimized values, F and P_{11} , the spectral reflectance factor of the cyan ramp samples were reconstructed. The average RMS reflectance error was 0.01023. The measured and reconstructed spectral reflectance curves are shown in Figure 2. And it shows the reconstructed curves corresponding to small F value except $F=0$ have large RMS errors. These errors are caused by the difference between an assumed ideal dot shape and an actual dot shape.

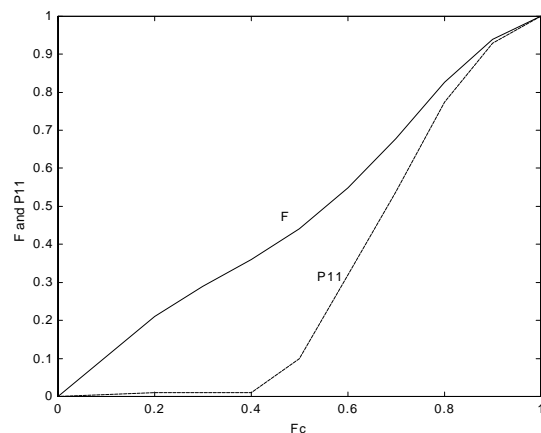


Figure 1. Predicted F (solid line) and P_{11} (dotted line)

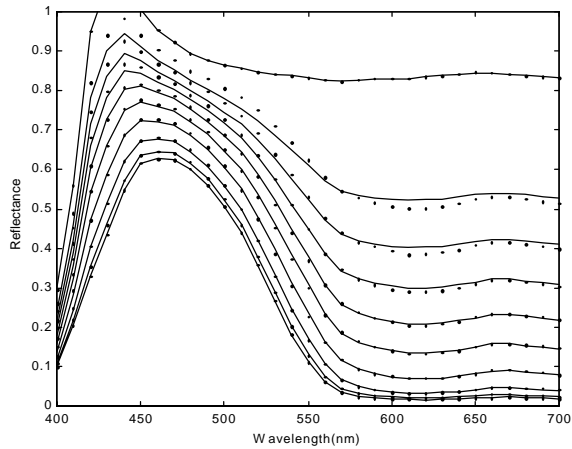


Figure 2. Measured spectral reflectance factor(dots) and predicted spectral reflectance factor(solid lines) of the cyan ramp

Toner Layer Thickness

This model assumes the toner layer thickness is uniform throughout the dot region and doesn't change depending on dot size as illustrated in Figure 3 (a). Practically, the actual dot doesn't have the ideal shape, as shown in Figure 3(b). Concerning the dot shape problem, Arney, Endeldrum, and Zeng suggested a model using a v factor.^{2,5} However, because the v factor was empirical value, we took another approach.

We assumed the toner layer thickness was not uniform and changed depending on F_c value, as shown in Figure 3(b). However, we used only the average toner thickness, because handling such not uniform thickness in the model was not easy. XR1 was introduced in the model. XR1 is a ratio of the average thickness to the thickness at $F_c=1$. Because x in Eq. 8 is the thickness at $F=1$, Sx_1 which was derived for the ink region by Eq. 8 is multiplied by XR1. XR1 varies depending on F_c value, but this value doesn't vary depending on the wavelength. Therefore, XR1 can be optimized using the nonlinear optimization with F and P_{11} .

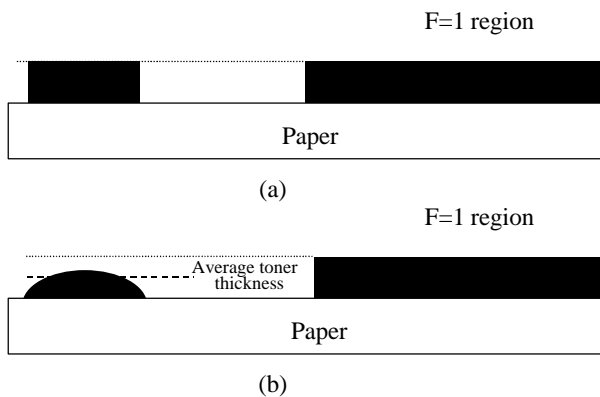


Figure 3. Ideal dot shape(a) and actual dot shape(b)

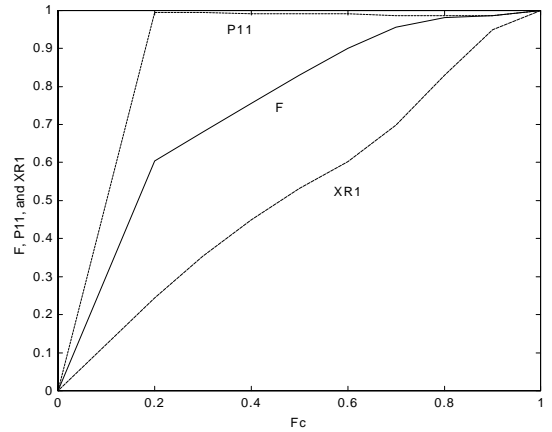


Figure 4. Predicted F (solid line), P_{11} (dashed line), and $XR1$ (dotted line)

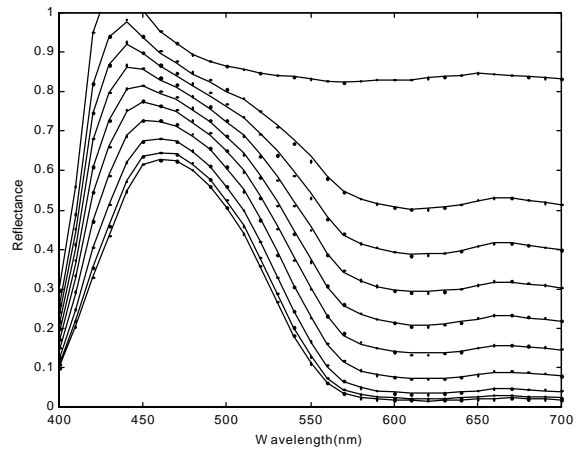


Figure 5. Measured spectral reflectance factor(dots) and predicted spectral reflectance factor(solid lines) of the cyan ramp

Because of strong mutual dependence between F , P_{11} , and $XR1$, this optimization had also a lot of local minimum values. The optimization method was similar to previous one, except about $XR1$. In order to save time, the optimum $XR1$ was derived for each combination of F and P_{11} using golden section search and parabolic interpolation in MATLAB function without adding to combination.

Figure 4 shows optimized F (solid line), P_{11} (dotted line), and $XR1$ (dashdot line). Using Eq. 1, Eq. 11, Eq. 12, and the optimized values, F , P_{11} , and $XR1$, the spectral reflectance factor of the cyan ramp samples were reconstructed. The average RMS reflectance error was 0.00373. The measured and reconstructed spectral reflectance curves are shown in Figure 5. And it shows the two curves are pretty close.

Comparison of predicted F value to measured F value

We obtained a good result about reconstructed curves. However, the predicted F values seem too high. And P_{11} is also too high. In order to check how closely the model can predict physical values, actual dot areas were measured by

the microdensitometer and were compared with the predicted F values.

Three samples, $F_c=0.3$, 0.5, and 0.7, were measured, and the halftone dot fractions, F_m , were estimated by a histogram analysis.⁷ The results are shown in Table 1. The F_m values corresponding to $F_c=0.3$ and 0.5 were lower than the predicted one.

This difference seems to be due to some approximations remaining in the model, for example, the uniformity of toner layer thickness, and also some errors included in the experimental data. Therefore, the parameters, which indicate the minimum RMS reflectance error, are not necessarily close to the physical values. The RMS reflectance errors, when the F value varied and the other parameters, P_{11} and $XR1$, were optimized with the varied F value, were calculated. They are shown in Figure 6. It is shown that only the F values within limited ranges can reach very small RMS reflectance error. Existence of the ranges seems to be due to the strong mutual dependence between three parameters, F , P_{11} , and $XR1$. Although the measured F values didn't agree with predicted values, they were included within the ranges.

Table 1. Predicted F and Measured F_m

F_c	0.3	0.5	0.7
Predicted F	0.680	0.830	0.955
Measured F_m	0.465	0.728	0.966

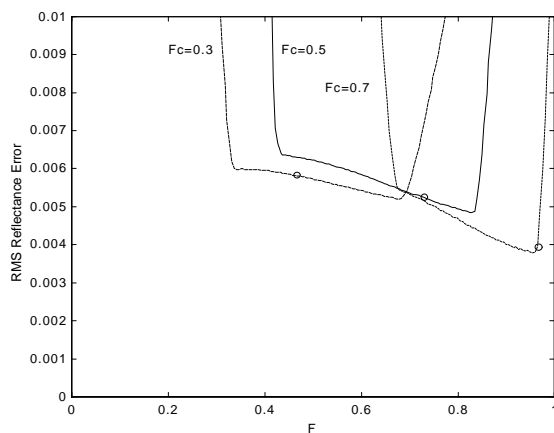


Figure 6. Variation of F value v.s. RMS reflectance error, $F_c=0.3$ (dotted line), $F_c=0.5$ (solid line), and $F_c=0.7$ (dashed line). Circles are measured F value

Conclusion

We attempted to optimize the parameters for the probability model using only the macroscopic spectral reflectance data. By introducing toner layer thickness parameter to the model, good fit between the measured and reconstructed spectral curves was obtained. Unfortunately, we have not reached to establish the optimization method without the microdensitometry. In the cause of the strong mutual dependence between the parameters, an obscurity of the model, and the error of data, there are many good combinations of the parameters for the reconstruction of the close spectral curve, and the method to select the best combination to express real physical structure has not found yet. However, it could be confirmed that the best parameter to express the physical structure was included within the good combinations for spectral curve fit.

Acknowledgements

We would like to thank Prof. R. S. Berns and Prof. J. S. Arney for their advice. We also acknowledge Dr. E. N. Dalal, K. M. Natale-Hoffman, and Y. Shapiro for measurements and valuable discussion with them.

References

1. J. R. Huntsman, *J. Imag. Technol.*, **41**, 136 (1987).
2. J. S. Arney, P. G. Engeldrum, and H. Zeng, *J. Imag. Sci. Technol.*, **39**, 502 (1995)
3. J. S. Arney, *J. Imag. Sci. Technol.*, **41**, 633 (1997).
4. J. S. Arney and S. Yamaguchi, submitted to *J. Imag. Sci. & Technol.* October 1998.
5. J. S. Arney and A. Tsujita, submitted to *J. Imag. Sci. & Technol.* October 1998.
6. D. B. Judd and G. Wysecki, *Color in Business, Science & Industry*, 3rd ed., John Wiley and Sons, Inc., New York, 1975 420
7. J. S. Arney and Yat-Ming Wong, *Histograms Analysis of the Microstructure of Halftone Images, IS&T's 1998 PICS Conference*, 206 (1998)